ORIGINAL ARTICLE

Journal
the American Ceramic Society

Atomic layer deposition of GDC cathodic functional thin films for oxide ion incorporation enhancement

Hwichul Yang[1] (iD) | Hojae Lee[1] | Yonghyun Lim[1] | Young-Beom Kim[1,2] (iD)

[1]Department of Mechanical Convergence Engineering, Hanyang University, Seoul, Republic of Korea

[2]Institute of Nano Science and Technology, Hanyang University, Seoul, Republic of Korea

Correspondence
Young-Beom Kim, Department of Mechanical Convergence Engineering, Hanyang University, 222 Wangsimni-ro, Seongdong-gu, Seoul 04763, Republic of Korea.
Email: ybkim@hanyang.ac.kr

Abstract

In this paper, we report successful fabrication of a gadolinia-doped ceria (GDC) thin film using atomic layer deposition (ALD) for improving the performance of solid oxide fuel cells (SOFCs). By varying the deposition conditions and adjusting the configuration of the ALD supercycle, the doping ratio of ALD GDC was controlled. The morphology, crystallinity, and chemical composition of ALD GDC thin films were analyzed. ALD GDC showed different surface chemistry, including oxidation states, at different doping ratios. The application of ALD GDC in a SOFC led to an output power density enhancement greater than 2.5 times. With an anodic aluminum oxide (AAO) porous support structure, an ALD GDC thin film SOFC (TF-SOFC) showed a high power density of 288.24 mW/cm^2 at an operating temperature of 450°C.

KEYWORDS

atomic layer deposition, functional interlayer, Gadolinia-doped ceria, low-temperature solid oxide fuel cells, oxide ion incorporation

1 | INTRODUCTION

Fuel cells are considered one of the most promising renewable energy technologies for addressing the lack of conventional energy resources, such as fossil fuels, in the current era. Among the various types of fuel cells, solid oxide fuel cells (SOFCs) are of particular interest due to their high efficiency for energy conversion, lack of pollutant emission, and fuel flexibility. Typical SOFCs operate at high temperatures (800-1000°C), which hinders wide range of practical applications and this high-temperature operation also leads to thermal management problems and high system costs as well as accelerated performance degradation. In past decades, many studies were conducted to reduce SOFC operating temperature, and these efforts succeeded at lowering the operating temperature to less than 500°C.[1-5] However, low-temperature SOFCs (LT-SOFCs) have several unresolved technological challenges: (a) sluggish ionic conduction in the solid oxide electrolyte at low temperature and (b) sluggish surface charge transfer reactions due to decreased catalytic activity.[5]

At low temperatures, ionic conduction through solid oxide electrolyte becomes sluggish.[6] To compensate, there are two major approaches. One method adopts a highly oxygen-ion-conductive material, such as acceptor doped ceria (CeO$_2$), as an electrolyte instead of typical electrolytes, such as yttrium-stabilized zirconia (YSZ). The other technique entails thin film application of the electrolyte.[7-10] Decreasing electrolyte thickness with thin film fabrication methods results in shortened ionic conduction path. Thus, a thin electrolyte minimizes fuel cell loss from ionic conduction in the electrolyte. To adopt a thin film electrolyte, a supporting structure is necessary to provide mechanical strength to the thin film. For this purpose, anodic support structures, such as Ni-YSZ (yttria-stabilized zirconia) composite anodes and anodized aluminum oxides (AAO), have been widely used.[11,12] These support structures must be porous for fuel permeability, but this porosity leads to the pin-hole problem in the electrolyte. The thin electrolyte has to be dense to avoid an electrical short between the anode and cathode; therefore, vacuum-based thin film fabrication methods, including sputtering, pulsed laser

deposition (PLD), and chemical vapor deposition (CVD), have been widely used to fabricate dense thin films thinner than a few tens of micrometers. Research and development efforts using the various thin film fabrication techniques have yielded TF-SOFC electrolyte thicknesses on the order of a few tens of nanometers, thereby minimizing loss from ionic conduction in the electrolyte and improving the performance of SOFCs at low operating temperature.

Although adoption of thin film electrolytes significantly reduces ohmic loss, sluggish oxygen reduction reaction (ORR) kinetics at low temperature remains a challenge that adversely affects LT-SOFC performance. In the low-temperature regime, a low rate of oxygen ion incorporation into the surface of the electrolyte slows the ORR kinetics. To secure improved performance of LT-SOFCs, it is important to promote oxygen ion incorporation and, subsequently, ORR kinetics. In many studies, a cathodic functional layer (CFL) has been inserted between the cathode and electrolyte to enhance surface ORR kinetics.[13-18] As a functional material for this application, CeO_2-based materials have been introduced for their high rates of oxygen ion incorporation through high surface exchange kinetics and high oxygen ion conductivity. In particular, CeO_2 materials doped with acceptors such as yttrium (Y), gadolinium (Gd), and samarium (Sm) have been extensively researched. Studies have demonstrated higher surface kinetics for these materials than YSZ and enhanced performance.

In addition, thin film characteristics including surface grain boundary density are also important for enhancing ORR kinetics at the cathode/electrolyte interface. Grain boundary at the surface has been known as a favorable site for oxygen ion incorporation, and there has been researches that investigate this characteristic.[19,20] Also, Hong et al reported that a grain-controlled layer (GCL), which is a layer with well-developed grains, enhanced the performance even when the material for GCL was the same as the main electrolyte.[21,22] These researches demonstrated that it is important to fabricate thin films with high grain boundary density for improvement of the functional layer characteristics.

Atomic layer deposition (ALD) is a vacuum-based, state-of-art thin film fabrication technique. It is capable of depositing thin films composed of various materials, precisely controlling film composition and thickness, and obtaining conformal thin films with superior density even on complex structures (ie 3-D structures).[8,23,24] Atomic layer deposition has been applied to surface modification of electrolyte interface which contacts with the cathode for enhancing the ORR kinetics.[13-15,25] Fan et al used ALD to obtain conformal thin films of yttria-doped ceria (YDC) with thicknesses of tens of nanometers.[15] In addition, Y_2O_3 doping ratio in the YDC thin film could be controlled by adjusting ALD deposition recipe.[14] Thus, the ALD technique can be leveraged for improving surface oxygen kinetics through its ability to deposit

thin and conformal films on the entire surface of an electrolyte and its ability to control film composition to optimize its characteristics for ORR. However, there is limited research regarding ALD fabrication of other ceria-based materials.

In this study, we report ALD fabrication of gadolinia-doped ceria (GDC) thin films and their application to cathodic functional layer of LT-SOFCs. In addition, optimal doping ratio of gadolinia was also investigated coupled with the surface kinetics improvement. GDC has both high ionic conductivity and superior ORR kinetics than YSZ. Despite the beneficial characteristics of GDC for application in SOFCs, there have been few attempts reported to fabricate GDC using ALD. To the best of our knowledge, this is the first practical study of ALD GDC fabrication for application to SOFCs. We successfully fabricated GDC thin films via ALD and evaluated their material characteristics, including micro-structure, crystallinity, and electrochemical performances. By adjusting the deposition cycle configuration of the ALD process, we varied the composition of ALD GDC to find the optimal composition for SOFC functional interlayer applications. Finally, we adopted ALD GDC in a membrane-electrode-assembly (MEA), composed of an anode support structure and YSZ electrolyte, and demonstrated enhanced ORR kinetics with high fuel cell performance in terms of power density. The results in this study may provide implications not only in designing TF-SOFC structure for enhanced performance but also for other energy conversion and storage devices using thin films.

2 | MATERIALS AND METHODS

2.1 | Synthesis of atomic layer deposited GDC

For ALD GDC thin film fabrication, a flow-type ALD system with a quartz tubular chamber (IH-10, I TECH U Co., ltd) was used. The chamber was heated by a tube furnace to maintain constant temperature. During the deposition process, the working pressure of the chamber was maintained at 0.450 Torr with a mechanical rotary pump. The precursors and oxidant were delivered to the chamber by argon carrier gas (99.999% purity) supplied to the chamber at a constant flow rate. Tris(2,2,6,6-tetramethyl-3,5-heptanedionato)gadolinium [Gd(TMHD)$_3$] and tetrakis(2,2,6,6-tetramethyl-3,5-heptanedionato)cerium [Ce(TMHD)$_4$] (Strem Chemicals, Inc) were used for deposition of Gd_2O_3 and CeO_2, respectively. Ozone, which is highly reactive, was used as the oxidant due to the low reactivity of Gd and Ce precursors at the ALD process temperature and was generated and controlled using a pure O_2 gas (99.995% purity) ATLAS ozone generator (AbsoluteOzone®). The concentration of generated ozone was maintained at 20 wt%, which was monitored by a

TABLE 1 Summary of atomic layer deposition (ALD) gadolinia-doped ceria (GDC) parameters: supercycle configuration, deposition rate per supercycle, and deposition cycles

Recipe	Supercycle configuration						Deposition rate (Å/supercycle)	Number of cycles	Actual thickness (nm)
GDC 2:1	Ce	Ce	Gd				1.755	170	26.43
GDC 3:1	Ce	Ce	Ce	Gd			2.505	130	28.15
GDC 4:1	Ce	Ce	Ce	Ce	Gd		3.255	100	26.26
GDC 5:1	Ce	Ce	Ce	Ce	Ce	Gd	4.005	85	29.78

full flow ozone sensor (IN USA, Inc). The temperature of the chamber was varied from 250 to 300°C to achieve the desired deposition rate of each material. The precursor containers were heated to 190 and 230°C for the Gd and Ce precursors, respectively. A deposition cycle of Gd_2O_3 and CeO_2 consists of four steps: a precursor pulse [3 seconds for $Gd(TMHD)_3$ and 2 seconds for $Ce(TMHD)_4$], Ar purging (30 seconds), an oxidant pulse (5 seconds), and Ar purging (30 seconds). The deposition rate at 250°C is 0.255 Å/cycle for Gd_2O_3 and 0.75 Å/cycle for CeO_2. For deposition of GDC, individual cycles were performed at various ratios to form a super-cycle for GDC. Approximately 30-nm-thick ALD GDC thin films were controllably synthesized by adjusting the number of super-cycles used in the fabrication process.

2.2 | Thin film characterization and electrochemical analysis

ALD GDC was coated onto a single crystalline (100) silicon wafer substrate for thin film characterization. Microstructural analysis of the thin film was performed with a field emission-scanning electron microscope (FE-SEM, S-4800, Hitachi) and an atomic force microscope (AFM, XE-70, Park Systems). Chemical composition and crystallinity were analyzed using an X-ray photoelectron spectrometer (XPS, Theta Probe, Thermo Fisher Scientific Co.) and an X-ray diffractometer (XRD, SmartLab, Rigaku).

For evaluation of electrochemical performance, a polycrystalline YSZ (yttria-stabilized zirconia, 8 mol%-doped) substrate with one side polished and 200 μm thickness was used. ALD GDC was coated onto the polished side of the YSZ substrate, which is the cathode side. Platinum (Pt) electrodes were fabricated by direct current (DC)-magnetron sputtering for both the anode and cathode. For high-performance fuel cells fabrication with ultra-thin electrolyte incorporating ALD GDC functional layer, a porous anodic aluminum oxide (AAO) substrate with 50 nm pores (InRedox LLC) was used as a mechanical support membrane. A combinatorial Pt anode was deposited on the AAO substrate and was coated with a sputtered YSZ thin film electrolyte.[12] Additional ALD GDC thin film was then deposited on the YSZ electrolyte. Finally, a porous Pt cathode fabricated by

sputtering was placed on the ALD GDC. Detailed microstructure of the thin-film SOFC was observed by field emission transmission electron microscope (FE-TEM). Fuel cell operating characterization by linear sweep voltammetry (LSV) and electrochemical impedance spectroscopy (EIS) were performed with an electrochemical analyzer (reference 600, Gamry Instruments) utilizing a home-made fuel cell test station. During the fuel cell characterization, the temperature of the test station was maintained between 350 and 450°C, and pure H_2 gas (99.999%) was supplied as a fuel. LSV was conducted in the voltage range from the open circuit voltage to 0.2 V to obtain current-voltage behavior, and EIS was conducted in the frequency range from 1 MHz to 1 Hz. The obtained data from EIS were fitted and analyzed by an equivalent circuit model.

3 | RESULTS AND DISCUSSION

Table 1 summarizes the supercycle configurations used for ALD GDC deposition. The recipes for ALD GDC films consisted of 2 to 5 cycles of CeO_2 deposition combined with 1 cycle of Gd_2O_3 deposition. Using the measured individual deposition rates of CeO_2 and Gd_2O_3, the deposition rate per supercycle was calculated. Z. Fan et al reported that a functional layer fabricated with ALD covers the entire surface and shows optimal performance when its thickness is >10 nm.[26] The number of deposition cycles was adjusted to obtain a thickness exceeding the critical thickness, and the actual thicknesses of the ALD GDC thin films were measured. The thickness of each sample was about 30 nm, enough to cover the surface of YSZ substrate for characterization of SOFC performance (Figure 1).

Figure 2 shows the surface morphology of the GDC 3:1 sample. All of the ALD GDC samples possess similar surface characteristics. As shown in Figure 2A, the ALD GDC thin film had nano grains that resulted in determination difficulty of exact grain sizes. For detailed analysis of the surface, AFM measurement was conducted. The AFM topography (Figure 2B) results support the SEM data and reveal the roughness of the surface. The RMS surface roughness (R_q) was measured as 0.420 nm indicating a surface area increase rate of only 0.1235%. These data show that the surfaces of

FIGURE 1 (A) Atomic layer deposition of gadolinia-doped ceria (GDC). Schematics of a fuel cell with an ALD GDC functional layer on (B) yttrium-stabilized zirconia substrate and (C) anodized aluminum oxides porous supporting substrate [Color figure can be viewed at wileyonlinelibrary.com]
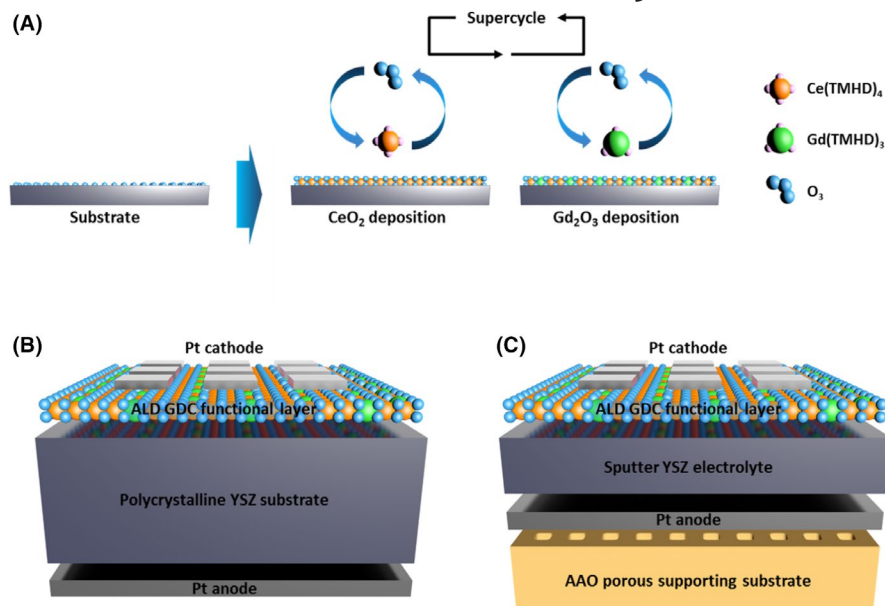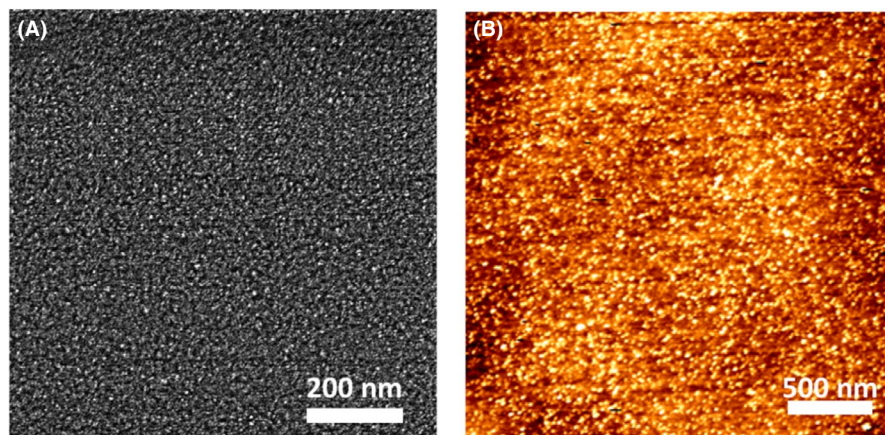

FIGURE 2 (A) Scanning electron microscope image of atomic layer deposition gadolinia-doped ceria (GDC) deposited on a Si substrate. (B) Surface topography image (2.5 μm × 2.5 μm) by atomic force microscope. The images were acquired from the GDC 3:1 sample [Color figure can be viewed at wileyonlinelibrary. com]

the ALD GDC thin films are essentially flat and it also can be suggested that the SOFC performance enhancement via ALD GDC functional layer is due to the material properties of ALD GDC, not the geometric effect which means the active area enhancement by roughness.

The crystalline phases of the thin film by XRD measurement are shown in Figure 3. From the XRD spectrum obtained from the ALD GDC 3:1 sample, several peaks that correspond to cubic fluorite phase of GDC were observed. The predominant peaks exhibited by the ALD GDC thin film correspond to the (111), (200), (220), and (311) planes, and minor peaks corresponding to the (222), (400), (331), and (420) planes were also observed. There was no Si(100) substrate peak because the XRD measurement was conducted under grazing incidence XRD (GI-XRD) mode. When the ALD deposition temperature was relatively high (>100-200°C), crystalline peaks were observed in XRD spectrum of the ALD thin film.[27] Also, for CeO_2 deposition, a cubic crystalline structure develops when fabricated at 175-250°C.[28]
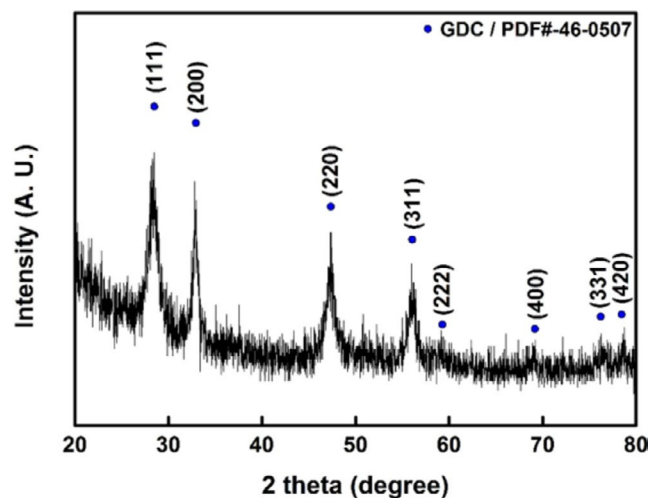

FIGURE 3 Representative x-ray diffractometer spectrum of atomic layer deposition (ALD) gadolinia-doped ceria (GDC) thin film on Si substrate. The data were obtained from the ALD GDC 3:1 sample [Color figure can be viewed at wileyonlinelibrary.com]

Deposition of ALD GDC was conducted at a substrate temperature of 250°C; thus, the ALD GDC thin films developed a crystalline structure. The characterization data showed that the ALD GDC thin films were composed of small grains of cubic fluorite phase.

Diverse doping level of gadolinium oxide into ceria provides different surface activity for oxygen incorporation. Figure 4 shows doping ratios of ALD GDC resulting from different CeO_2 and Gd_2O_3 cycle ratios. As summarized in Table 1, the ALD cycle ratios between CeO_2 and Gd_2O_3 were adjusted from 5:1 to 2:1 in this experiment. The doping ratio for each cycle ratio was estimated using the deposition rate of each material and the rule of mixture (ROM), which is used for calculating the composition of compound materials.[29] The estimated value of Gd_2O_3 mol% for the ALD GDC samples ranged from 10 to 25 mol%. Doped-ceria materials show optimal characteristics for SOFC at doping ratios from 12 to 17 mol%.[14] Thus, the ALD cycle ratio was set from 5:1 to 2:1 to obtain a thin film with a composition in this range. Using the atomic composition of each element from the XPS measurements, the experimental Gd_2O_3 mol% was determined. The measured Gd_2O_3 doping ratios were 11.9, 13.9, 18.8, and 25.2 mol% for the GDC 5:1, 4:1, 3:1, and 2:1 samples, respectively. As shown in Figure 4, the measured values well followed the trend of the estimated values. Thus, the composition of GDC was well-controlled by the ALD process.

To investigate the characteristics related to the doping ratio of ALD GDC, detailed XPS spectra were obtained from the surface of the ALD GDC films (Figure 5A-D). The O1s spectrum provides information about the surface chemistry of the samples, including oxidation state.[30,31] The spectra can
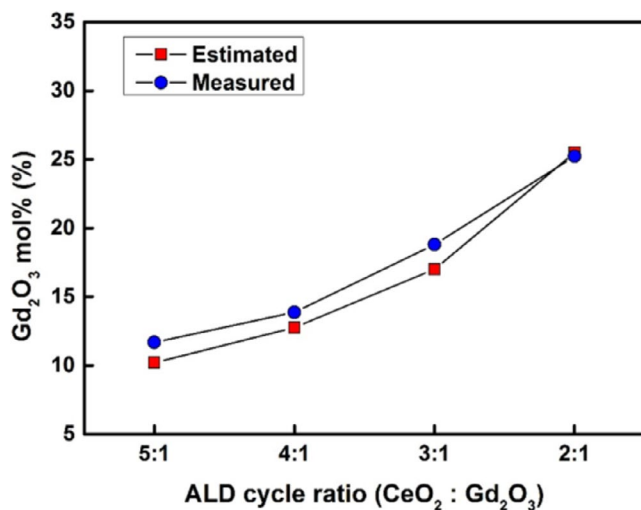

FIGURE 4 Doping ratios of atomic layer deposition (ALD) gadolinia-doped ceria with respect to ALD recipe as measured by x-ray photoelectron spectrometer (XPS). Red squares represent the calculated value estimated using the deposition rates of CeO_2 and Gd_2O_3, and blue circles represent the value calculated from the XPS-measured data [Color figure can be viewed at wileyonlinelibrary.com]

be deconvoluted into three peaks with binding energies at approximately 529, 531, and 534 eV; these peaks correspond to oxygen in the lattice oxide (O^{2-}), in hydroxyl groups (-OH), and in adsorbed water, respectively. The peaks near 534 eV were negligible for all samples, while the other two peaks were relatively strong. As the CeO_2 cycle ratio increased, the intensity of the O^{2-} peak near 529 eV increased, while the intensity of the –OH peak near 531 eV decreased. The intensity ratios of the O^{2-} ($I_{lattice}$) peak to the –OH (I_{-OH}) peak for the different ALD cycle ratios are shown in Figure 5E. This intensity ratio decreased as the relative number of CeO_2 deposition cycles per supercycle decreased. If the $I_{lattice}/I_{-OH}$ ratio is high, then the oxidation state is high.[30,31] For a doped-ceria system, the high oxidation state means that cerium cations exist in the form of Ce^{4+}. As shown in Figure 5E, the surface oxidation state decreases as ALD cycle ratio decreases from 5:1 to 2:1. Ce3d XPS spectra (Figure S2) also provided information about the redox state of Ce. Reduction of Ce^{4+} to Ce^{3+} by gadolinium doping forms oxygen vacancies in the doped-ceria system that act as sites for ion conduction and surface exchange reactions.[1,14] Thus, the lower the CeO_2 deposition ratio of the ALD recipe, that is, the larger the amount of gadolinium doping, the higher the number of sites available for the oxygen surface exchange reaction. In application of an ALD GDC thin film as a cathodic functional layer, this capability is one of the major factors that determine the performance of SOFCs.

Fuel cell performances were measured and compared the enhancement effects with the different composition ALD GDC functional layers. Figure 6A shows the current-voltage (I-V) behavior of fuel cells at an operating temperature of 450°C with different electrolyte layers: bare YSZ substrate electrolyte (w/o GDC) and ALD GDC-applied electrolyte (ALD GDC 2:1 - 5:1). I-V behavior and power density varied depending on the ALD recipe used for ALD GDC deposition. While the bare YSZ substrate sample showed a maximum power density of 3.92 mW/cm², the ALD GDC-incorporated samples showed maximum power densities of 7.21, 9.23, 9.81, and 9.49 mW/cm² for the GDC 5:1, 4:1, 3:1, and 2:1 samples, respectively, which correspond to performance improvements by factors of 1.84, 2.35, 2.50, and 2.42. For all samples, the main electrolyte was a commercial 200-μm-thick YSZ substrate, and the ALD GDC layer was only about 30 nm thick. Therefore, these performance improvements stemmed from a decrease in electrode interface resistance rather than ionic transport resistance. Comparing the ALD GDC-incorporated samples, the power density increased monotonically as the ratio of CeO_2 in the ALD recipe decreased from 5:1 to 3:1. However, power density decreased in the ALD GDC 2:1 sample compared to the ALD GDC 3:1 sample. Thus, the optimum deposition recipe for ALD GDC is a CeO_2 to Gd_2O_3 ratio of 3:1, which corresponds to a Gd_2O_3 doping ratio of 18.8 mol% (Figure 4). The optimal doping ratio of GDC is slightly higher than that for YDC, which is about 14 mol%.[14,15]
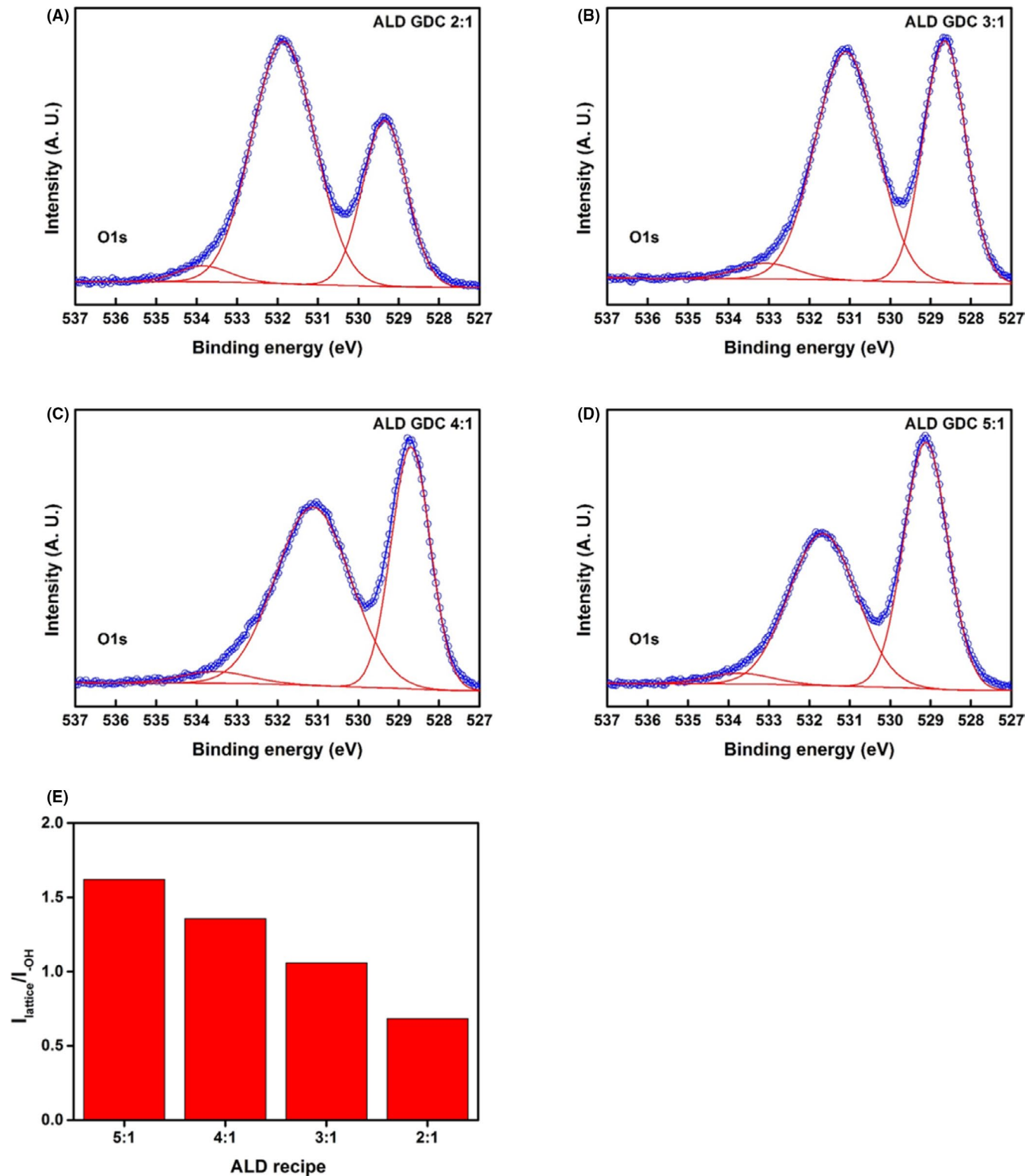
FIGURE 5 O1s x-ray photoelectron spectrometer spectra of atomic layer deposition gadolinia-doped ceria films fabricated with doping ratios of (A) 2:1, (B) 3:1, (C) 4:1, and (D) 5:1. Each spectrum was deconvoluted into three peaks. The measured data are depicted by blue line and circles, and the deconvoluted peaks are represented with red lines (E) Intensity ratio of oxygen in the lattice oxide ($I_{lattice}$) peak to and oxygen in the –OH group (I_{OH}) peak for each doping ratio [Color figure can be viewed at wileyonlinelibrary.com]

From the oxidation state information provided by the O1s XPS spectral analysis (Figure 5), we suggest that there are more sites for oxygen surface exchange reactions at the ALD GDC surface when gadolinium doping increases up to 18.8 mol%. Several studies have reported that excessive doping may reduce the characteristics associated with oxygen ion incorporation and
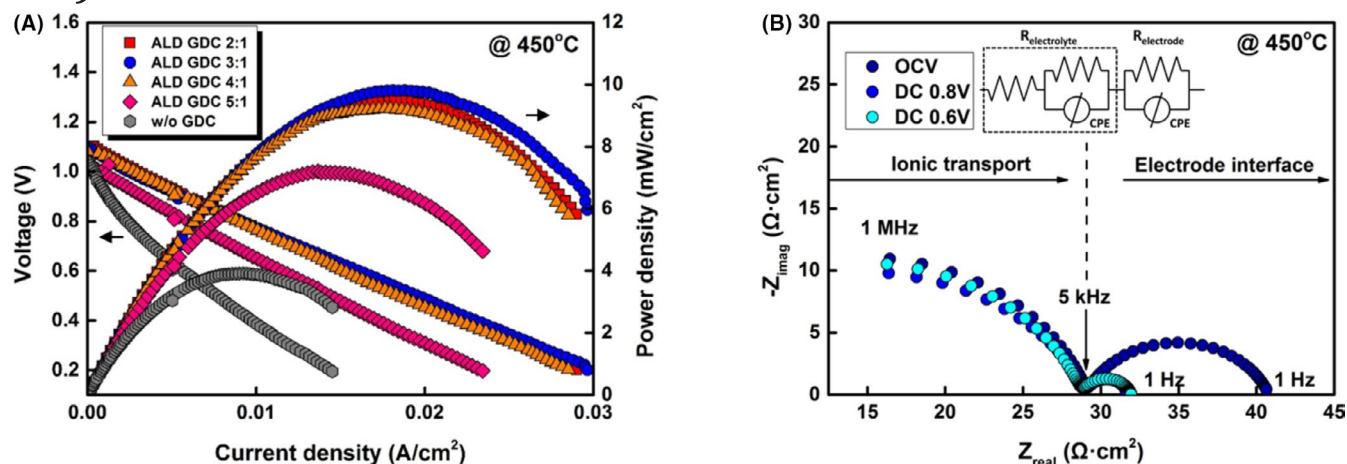
FIGURE 6 (A) Current-voltage (I-V) curves and power density of solid oxide fuel cells composed of yttrium-stabilized zirconia substrate and gadolinia-doped ceria (GDC) functional layers fabricated by atomic layer deposition (ALD) with various recipes. (B) Representative EIS spectra of the ALD GDC 3:1 sample for different bias voltages. The data were fitted with an equivalent circuit (inset). These data were measured at 450°C [Color figure can be viewed at wileyonlinelibrary.com]
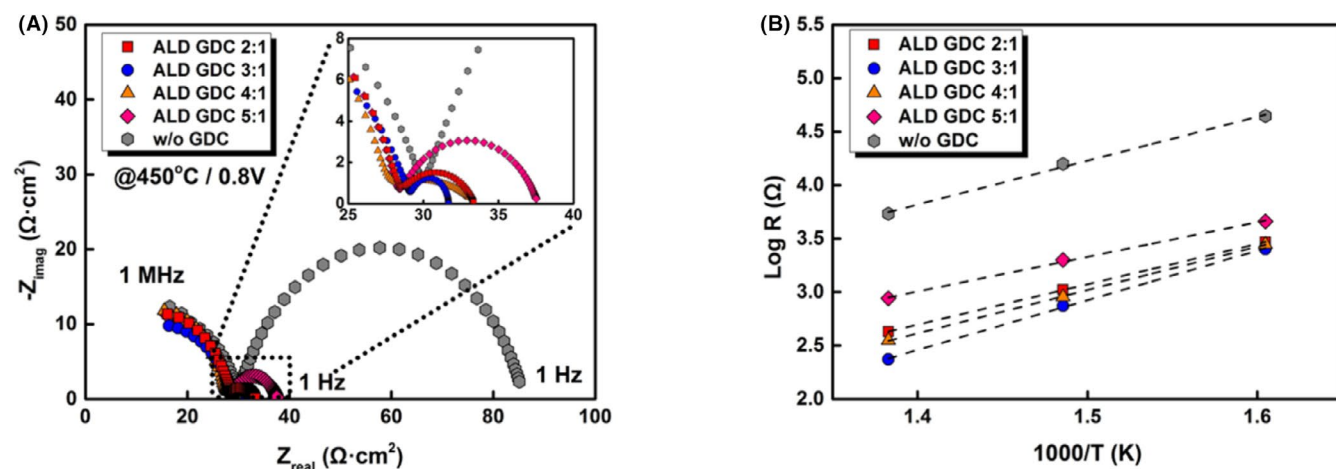

FIGURE 7 (A) Electrochemical impedance spectroscopy (EIS) spectra of solid oxide fuel cells composed of yttrium-stabilized zirconia substrate and atomic layer deposition gadolinia-doped ceria functional layers at 450°C and a bias voltage of 0.8 V. The inset plot is a magnified plot near the intersection of the graphs. (B) Arrhenius plot of the charge transfer resistance extracted from the EIS spectra at a bias voltage of 0.8 V and temperatures of 350, 400, and 450°C [Color figure can be viewed at wileyonlinelibrary.com]

surface exchange. Chao et al studied ALD YSZ with different molar ratios, and its surface exchange kinetics was optimized at a doping level of 14 mol%; YSZ characteristics worsened when doping was increased further.[25] In addition, ALD YDC, which is most similar material to the material in our study, showed optimal performance at a doping ratio of 14.1 mol%.[14] A possible explanation for these results is that the defects that act as oxygen ion incorporation sites can interact with each other when the defect concentration exceeds a certain level.[32] Therefore, based on previous researches, we conclude that excessive Gd_2O_3 doping may interfere with oxygen ion incorporation.

To further investigate the contributions of the performance improvement, EIS measurements were conducted in the frequency range from 1 MHz to 1 Hz at applied dc voltages of 0.6, 0.8 V, and OCV at various temperatures. Figure 6B

shows the representative EIS spectra for the ALD GDC 3:1 sample measured at 450°C. The spectra were the result of fitting with an equivalent circuit model shown in the inset of the figure. EIS spectra were composed of two semi-circles. The first semi-circle in the high frequency range from 1 MHz to about 5 kHz is independent of the bias voltage, indicating that it is related to the resistance from ionic transport. The second semi-circle in the low frequency range from 5 kHz to 1 Hz varied with bias voltage. This characteristic indicates that this semi-circle represents the resistance at the electrolyte/electrode interface. Figure 7A shows EIS spectra for each sample at 450°C and at a bias voltage of 0.8 V for comparison. While the size of the first semi-circle was similar for all samples, all ALD GDC samples showed a significant reduction in the size of the second semi-circle compared to the sample without

GDC. It is also evident that the size of the second semi-circle decreased as the CeO_2 ratio in the ALD GDC decreased from 5:1 to 3:1 but increased at a ratio of 2:1. This trend is identical to that shown by the current-voltage curves in Figure 6A. The electrode/electrolyte interface resistance represented by the size of the semi-circle at the bias voltage of 0.8 V and temperatures of 350, 400, and 450°C is shown in Figure 7B. ALD GDC samples had lower resistances by an order of magnitude than the sample without GDC. In particular, the ALD GDC 3:1 sample had almost a factor of 1.5 lower resistance. The results show that the performance improvement of ALD GDC SOFCs stemmed from reduction of electrode/electrolyte interface resistance and superior surface kinetics.

Through the Tafel approximation, we calculated the exchange current density (Figure S3), which is shown in Figure 8. The exchange current density represents the reaction speed and is used to indicate the activity of the surface kinetics.[33] The ALD GDC 3:1 sample showed an exchange current density of 4.72 mA/cm^2 at 450°C, which is almost 4.3-times higher than the 1.11 mW/cm^2 value for the sample without GDC. The exchange current density showed the same trend as the power density and resistance in the EIS spectra. In Figure 8, the slope of the dotted lines provides information about the activation energy of the electrode/electrolyte interface.[15] The activation energy of the sample without GDC was calculated to be 0.822 eV, while the ALD GDC 5:1, 4:1, 3:1, and 2:1 samples had activation energies of 0.722, 0.677, 0.626, and 0.646 eV, respectively. Thus, inserting an ALD GDC layer significantly reduced the activation energy of the electrode/electrolyte interface. These results provide an explanation to why incorporation of ALD GDC improved SOFC performance.

To evaluate the practical availability of ALD GDC, we fabricated a thin-film SOFC on a commercial AAO substrate with
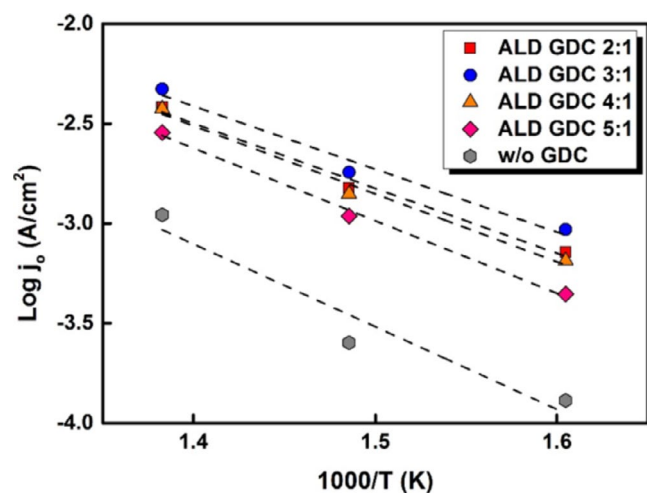

FIGURE 8 Arrhenius plot of the exchange current density at the interface between the atomic layer deposition gadolinia-doped ceria functional layers and the Pt cathode. The values were extracted from the Tafel approximation [Color figure can be viewed at wileyonlinelibrary.com]

a thin, sputtered YSZ electrolyte and an ALD GDC functional layer. The structure of the thin-film SOFC with ALD GDC functional layer is shown in Figure 9. The cross-sectional TEM image in Figure 9A and B shows bi-layered structure of YSZ and ALD GDC functional layer. The thickness of ALD GDC functional layer is about 50 nm, which is slightly higher than the results in Table 1, but it is negligible for ionic conduction due to relatively thick layer of sputtered YSZ main electrolyte and high ionic conductivity of GDC.[1,7] In Figure 9C, ALD GDC layer has a morphology with nano-sized grains. These tiny grains and lots of grain boundaries become sites for oxygen incorporation at the cathode side.[19,20] In addition, fast Fourier transform (FFT) pattern in Figure 9D confirmed the polycrystalline structure of ALD GDC. The FFT pattern shows mainly four ring patterns corresponding to (111), (200), (220), and (311) structure from the inside to outside (1-4 in the Figure 9D), respectively, and it is consistent with the XRD result in Figure 3. Figure 10 shows current-voltage behavior and EIS spectra of the AAO-supported SOFCs with and without an ALD GDC functional layer. As shown in Figure 10A, the AAO-supported SOFC with ALD GDC showed a greatly improved maximum power density of 288.24 mW/cm^2 compared to the 107.44 mW/cm^2 exhibited by the SOFC with only YSZ electrolyte. The superior characteristics of the ALD GDC functional layer enhanced the power density approximately 2.7-fold and the power density value is high considering that this is not the composite electrolyte case. Figure 10B shows a significant decrease of electrode/electrolyte interface resistance in the sample using ALD GDC, while the ionic transport resistance was essentially unchanged. Although the total thickness of the electrolyte increases due to insertion of the ALD GDC functional layer, there is no significant difference in the size of the first semi-circle.[22] This result is due to both the relatively small (~50 nm) thickness increment resulting from addition of ALD GDC compared to total YSZ thickness as shown in Figure 9A-B and the relatively high ionic conductivity of doped-ceria materials (over an order of magnitude higher) compared to YSZ.[1,7] Thus, there was a negligible increase of ionic transport resistance and a significant decrease of electrode/electrolyte interface resistance when the ALD GDC functional layer was applied.

4 | CONCLUSIONS

To improve the performance of SOFCs, many novel materials have been developed with appropriate characteristics for application in SOFCs. Doped-ceria materials are the most promising materials for enhancing the ORR rate at the cathode/electrolyte surface. In this study, we successfully fabricated GDC thin films for use as a cathodic functional layer with ALD, a state-of-art thin film fabrication technique. ALD-fabricated GDC thin films had flat surfaces and showed nanocrystalline characteristics. To find the optimal
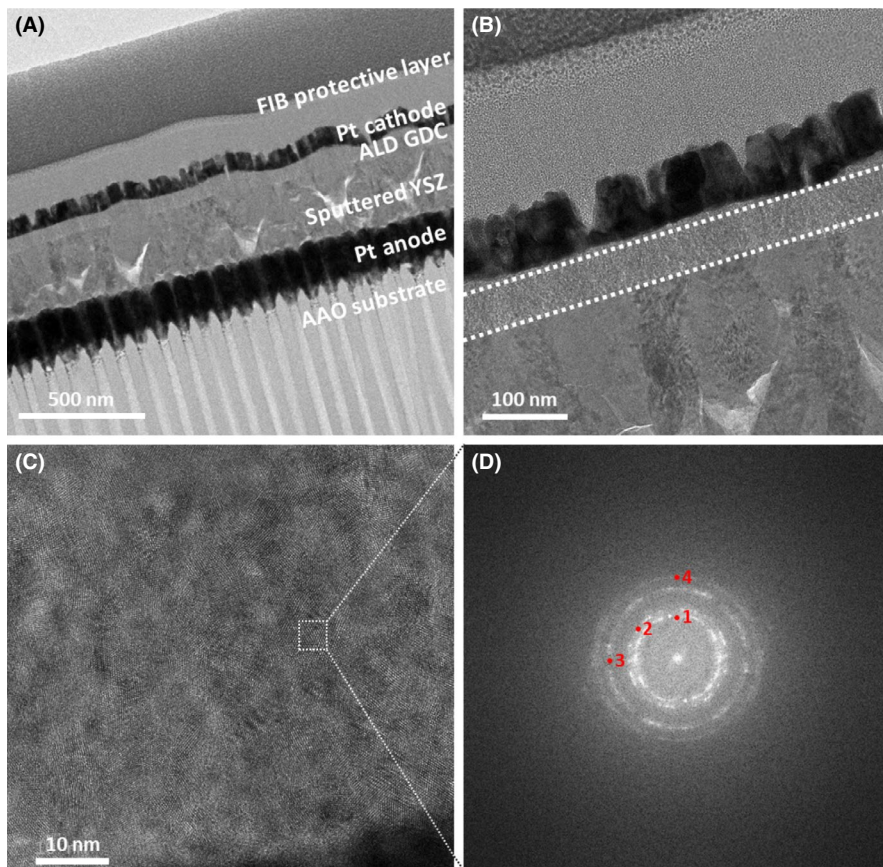
FIGURE 9 (A) Cross-sectional FE-TEM image of thin-film SOFC structure with atomic layer deposition (ALD) gadolinia-doped ceria (GDC) functional layer and (B) detailed view for ALD GDC functional layer. (C) High resolution FE-TEM image at the ALD GDC functional layer. (D) Fast Fourier transform pattern was achieved in the area indexed by white dotted line. Each number from 1 to 4 in the image corresponded to the GDC crystalline structure of (111), (200), (220), and (311), respectively [Color figure can be viewed at wileyonlinelibrary.com]
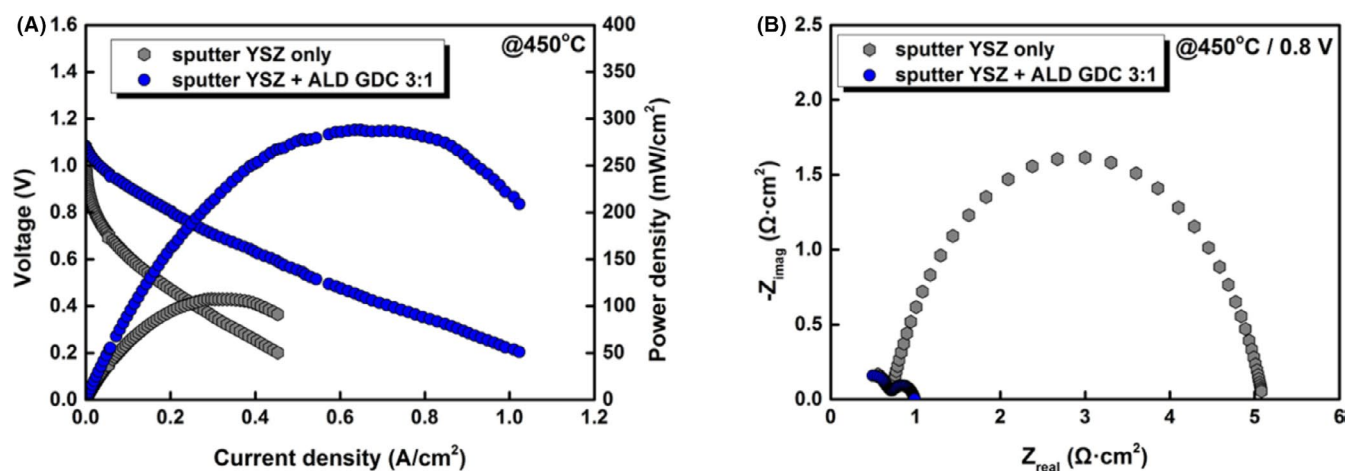

FIGURE 10 (A) Current-voltage (I-V) curves and power density of AAO-supported solid oxide fuel cells (SOFCs) with and without an atomic layer deposition gadolinia-doped ceria functional layer at 450°C. (B) Electrochemical impedance spectroscopy spectra of AAO-supported SOFCs at 450°C and a bias voltage of 0.8 V [Color figure can be viewed at wileyonlinelibrary.com]

doping ratio for GDC, ALD was conducted with various deposition conditions. Through XPS analysis, doping states and the resulting oxygen vacancy distribution at the surface of the ALD GDC thin films were analyzed. These properties are related to the ORR kinetics. We evaluated the impact of ALD GDC on SOFC performance and observed significant improvement in output power density. Incorporation of GDC with a doping ratio of 18.8 mol% enhanced performance by 2.5 times at an operating temperature of 450°C. We

fabricated an AAO supported thin film SOFC composed of a thin film YSZ electrolyte and ALD GDC functional layer, and analyzed the micro-structure of thin film SOFC configuration and ALD GDC layer with FE-TEM. For the thin film SOFC, application of ALD GDC showed a high power density of 288.24 mW/cm^2, which is a 2.7-times performance enhancement over the device fabricated without GDC. These results demonstrate the superior characteristics of ALD GDC for enhancing oxygen ion incorporation and ORR kinetics.

ORCID
Hwichul Yang https://orcid.org/0000-0002-6974-8696
Young-Beom Kim https://orcid.org/0000-0002-0307-0595

REFERENCES

1. Steele BCH. Oxygen transport and exchange in oxide ceramics. J Power Sources. 1994;49:1–14.
2. Doshi R, Richards VL, Carter JD, Wang X, Krumpelt M. Development of solid-oxide fuel cells that operate at 500°C. J Electrochem Soc. 1999;146(4):1273–8.
3. Xia C, Liu M. Novel cathodes for low-temperature solid oxide fuel cells. Adv Mater. 2002;14(7):521–3.
4. Zuo C, Zha S, Liu M, Hatano M, Uchiyama M. Ba(Zr0.1Ce0.7Y0.2)O3-d as an electrolyte for low-temperature solid-oxide fuel cells. Adv Mater. 2006;18:3318–20.
5. Wachsman ED, Lee KT. Lowering the temperature of solid oxide fuel cells. Science. 2011;334:935–40.
6. Skinner SJ, Kilner JA. Oxygen ion conductors. Mater Today. 2003;6:30–7.
7. Steele BCH. Appraisal of Ce1-yGdyO2-y/2 electrolytes for IT-SOFC operation at 500oC. Solid State Ionics. 2000;129:95–110.
8. Shim JH, Chao C-C, Huang H, Prinz FB. Atomic layer deposition of yttria-stabilized Zirconia for solid oxide fuel cells. Chem Mater. 2007;19:3850–4.
9. Noh H-S, Son J-W, Lee H, Song H-S, Lee H-W, Lee J-H. Low temperature performance improvement of SOFC with thin film electrolyte and electrodes fabricated by pulsed laser deposition. J Electrochem Soc. 2009;156(12):B1484–90.
10. Baek JD, Liu K-Y, Su P-C. A functional micro-solid oxide fuel cell with a 10 nm-thick freestanding electrolyte. J Mater Chem A. 2017;5:18414–9.
11. Leng YJ, Chan SH, Khor KA, Jiang SP. Performance evaluation of anode-supported solid oxide fuel cells with thin film YSZ electrolyte. Int J Hydrogen Energy. 2004;29:1025–33.
12. Hong S, Bae J, Koo B, Kim Y-B. High-performance ultra-thin film solid oxide fuel cell using anodized-aluminum-oxide supporting structure. Electrochem Commun. 2014;47:1–4.
13. Chao C-C, Kim YB, Prinz FB. Surface modification of yttria-stabilized Zirconia electrolyte by atomic layer deposition. Nano Lett. 2009;9(10):3626–8.
14. Fan Z, Chao C-C, Hossein-Babaei F, Prinz FB. Improving solid oxide fuel cells with yttria-doped ceria interlayers by atomic layer deposition. J Mater Chem. 2011;21:10903–6.
15. Fan Z, Prinz FB. Enhancing oxide ion incorporation kinetics by nanoscale yttria-doped ceria interlayers. Nano Lett. 2011;11:2202–5.
16. Kim YB, Holme TP, Gür TM, Prinz FB. Surface-modified low-temperature solid oxide fuel cell. Adv Func Mater. 2011;21:4684–90.
17. Bae J, Lee D, Hong S, Yang H, Kim Y-B. Three-dimensional hexagonal GDC interlayer for area enhancement of low-temperature solid oxide fuel cells. Surf Coat Technol. 2015;279:54–9.
18. Bae J, Yang H, Son J, Koo B, Kim Y-B. Enhanced oxygen reduction reaction in nanocrystalline surface of samaria-doped ceria via randomly distributed dopants. J Am Chem Soc. 2016;99(12):4050–6.
19. Shim JH, Park JS, Holme TP, Crabb K, Lee W, Kim YB, et al. Enhanced oxygen exchange and incorporation at surface grain boundaries on an oxide ion conductor. Acta Mater. 2012;60:1–6.
20. Lee W, Jung HJ, Lee MH, Kim Y-B, Park JS, Sinclair R, et al. Oxygen surface exchange at grain boundaries of oxide ion conductors. Adv Func Mater. 2012;22:965–71.
21. Hong S, Lim Y, Yang H, Bae J, Kim Y-B. Single-chamber fabrication of high-performance low-temperature solid oxide fuel cells with grain controlled functional layers. J Mater Chem A. 2017;5:2029–36.
22. Hong S, Son J, Lim Y, Yang H, Prinz FB, Kim Y-B. A homogeneous grain-controlled ScSZ functional layer for high performance low-temperature solid oxide fuel cells. J Mater Chem A. 2018;6:16506–14.
23. An J, Kim Y-B, Park J, Gür TM, Prinz FB. Three-dimensional nanostructured bilayer solid oxide fuel cell with 1.3 W/cm^2 at 450°C. Nano Lett. 2013;13:4551–5.
24. Johnson RW, Hultqvist A, Bent SF. A brief review of atomic layer deposition: from fundamentals to applications. Mater Today. 2014;17(5):236–46.
25. Chao C-C, Park JS, Tian X, Shim JH, Gür TM, Prinz FB. Enhanced oxygen exchange on surface-engineered yttria-stabilized Zirconia. ACS Nano. 2013;7(3):2186–91.
26. Fan Z, An J, Iancu A, Prinz FB. Thickness effects of yttria-doped ceria interlayers on solid oxide fuel cells. J Power Sources. 2012;218:187–91.
27. Hausmann DM, Gordon RG. Surface morphology and crystallinity control in the atomic layer deposition (ALD) of hafnium and zirconium oxide thin films. J Cryst Growth. 2003;249:251–61.
28. Päiväsaari J, Putkonen M, Niinistö L. Cerium dioxide buffer layers at low temperature by atomic layer deposition. J Mater Chem. 2002;12:1828–32.
29. Pickrahn KL, Garg A, Bent SF. ALD of ultrathin ternary oxide electrocatalysts for water splitting. ACS Catalyst. 2015;5:1609–16.
30. Smith RDL, Prévot MS, Fagan RD, Trudel S, Berlinguette CP. Water oxidation catalysis: electrocatalytic response to metal stoichiometry in amorphous metal oxide films containing iron, cobalt, and nickel. J Am Chem Soc. 2013;135:11580–6.
31. Choi HJ, Han GD, Bae K, Shim JH. Highly active oxygen evolution on carbon fiber paper coated with atomic-layer-deposited cobalt oxide. ACS Appl Mater Interfaces. 2019;11:10608–15.
32. Nakamura A Jr, Wagner JB. Defect structure, ionic conductivity, and diffusion in yttria stabilized zirconia and related oxide electrolytes with fluorite structure. J Electrochem Soc. 1986;133(8):1542–8.
33. O'Hayre RP, Cha S-W, Colella WG, Prinz FB. Fuel cell fundamentals. Hoboken, NJJohn Wiley & Sons, Inc.; 2008.

SUPPORTING INFORMATION
Additional supporting information may be found online in the Supporting Information section.

How to cite this article: Yang H, Lee H, Lim Y, Kim Y-B. Atomic layer deposition of GDC cathodic functional thin films for oxide ion incorporation enhancement. *J Am Ceram Soc*. 2021;104:86–95. https://doi.org/10.1111/jace.17457